ELSEVIER

Thermochimica Acta 397 (2003) 5–12

thermochimica acta

www.elsevier.com/locate/tca

Conformational properties of multihemic cytochromes *c* from *Desulfuromonas acetoxidans*

M.T. Giudici-Orticoni [a], A.A. Makarov [b,c], V.M. Lobachov [b,c], I.I. Protasevich [b,c], D. Lexa [a], M. Bruschi [a,*]

[a] *Laboratoire de Bioénergétique et Ingénierie des Protéines, Institut de Biologie Structurale et Microbiologie-CNRS, 31 Chemin J. Aiguier 13402 Marseille Cedex, 20 France*

[b] *Engelhardt Institute of Molecular Biology, Russian Academy of Sciences, Vavilov street 32, Moscow 117984, Russia*

[c] *UPRESA CNRS 6032, Université de la Méditerranée, 13385 Marseille, France*

Received 17 December 2001; received in revised form 11 April 2002; accepted 11 April 2002

Abstract

In the classification of *c*-type cytochromes, the class III includes multihemic cytochromes *c* with low redox potential constituting the cytochrome c_3 superfamily. Most of the cytochromes described have been isolated from sulfate or sulfur reducing bacteria. We report here the comparison between two multihemic cytochromes, the newly characterized 50 kDa cytochrome from *Desulfuromonas acetoxidans* and the cytochrome c_7 from the same strain in order to contribute to understanding the relationships between members of this superfamily. The thermostability of these cytochromes was studied by circular dichroism (CD) and differential scanning calorimetry (DSC). The influence of the temperature on the redox potential was also investigated. The data clearly indicate the presence of two domains in 50 kDa cytochrome and a drastic loss of stability of cytochrome c_7 in comparison to cytochrome c_3. The results are discussed in the light of the structural properties of the cytochrome c_3 superfamily and two sub-groups in this family are proposed.

Keywords: Differential scanning calorimetry; Multihemic cytochrome *c*; Sulfur reducing bacteria

1. Introduction

The multihemic cytochromes described so far in sulfate and sulfur-reducing bacteria are associated with diverse respiratory modes involving the use of elemental sulfur or oxidized sulfur compounds as terminal acceptors. Characterized by bishistidinyl axial iron coordination and low redox potentials, they are classified as class III cytochromes [1] and exhibit no structural similarity with the other cytochrome *c* classes. Among them, the three-dimensional structure of the monomeric tetraheme cytochrome c_3 [2–3], the dimeric tetraheme cytochrome c_3 [4], the nine-heme cytochromes c_3 [5] from sulfate-reducing bacteria and the *D. acetoxidans* cytochrome $c_{551,5}$ formerly known as cytochrome c_7 [6–7] are precisely described. On the basis of the amino acid sequence of a high molecular mass cytochrome *c* (Mr 65600) containing 16

Abbreviations: CD, circular dichroism; DSC, differential scanning calorimetry; *DvH*, *Desulfovibrio vulgaris* Hildenborough; *Dn*, *Desulfomicrobium norvegicum*; Hmc, high molecular mass cytochrome

* Corresponding author. Tel.: +33-491-164-144; fax: +33-491-779-517.
E-mail address: bruschi@ibsm.cnrs-mrs.fr (M. Bruschi).

0040-6031/02/$ – see front matter
PII: S0040-6031(02)00227-7

hemes [8] and the X-ray crystallographic comparisons of multihemic cytochromes, we have proposed that all these cytochromes belong to the cytochrome c_3 superfamily and that they have a common ancestral origin [9].

Desulforomonas acetoxidans cytochrome c_7 is a small (68 amino acids), monomeric cytochrome *c* containing three hemes. Amino acid sequence and three-dimensional structure are highly homologous to the tetraheme cytochrome c_3 from *Desulfovibrio*, apart from the fact that heme II is absent from cytochrome c_7. Recently, the biochemical and redox properties of new cytochromes proposed to belong to class III have been described in *D. acetoxidans*. A monohemic 10 and 50 kDa cytochromes have been described by Bruschi et al. [10] and 50 and 65 kDa cytochromes have simultaneously been reported by Pereira et al. [11]. The characterization by electrochemistry, optical and EPR spectroscopies revealed the 10 kDa cytochrome *c* to be the first monohemic cytochrome *c* exhibiting a bishistidinyl axial coordination and a low redox potential (−200 mV) [10]. The 50 kDa cytochrome is described to contain four hemes of low potential (−200 to −380 mV) in [10] and six hemes covering a wide range of reduction potentials (+100 to −375 mV) in [11]. The 65 kDa cytochrome is purified as an oligomer of 250 kDa containing a 65 kDa subunit of eight hemes exhibiting redox potentials from +180 to −250 mV [11].

We report here the further characterization of the 50 kDa cytochrome and its comparison with the cytochrome c_7 from the same strain in order to contribute to the understanding of the relationships between members of this superfamily. We have used circular dichroism (CD), which provides information on the heme environment and protein secondary structure, redox titration, which gives further insight into the heme reactivity, and differential scanning calorimetry (DSC) that provides the parameters of protein denaturation and domain structure. The structural features, which may be relevant to the observed differences in the thermal unfolding of these polyheme cytochromes, have been analysed. A relation between the number of hemes versus the molecular weight, the presence of domains with a cytochrome c_3-like folding and the thermostability of these polyhemic structures will be analyzed.

2. Materials and methods

2.1. Microorganisms and culture growth procedure and protein purifications

D. acetoxidans strain 5071 was grown as previously described by Pfennig and Biebl [12]. The basal salt medium used contained 0.05% ethanol (carbon and energy source) and 0.2% DL-sodium malate (electron acceptor). Cells were grown in a 200 l fermenter (Chemap) starting with a 40 l inoculum of fresh culture. The maximal absorbance of $A = 0.4$ at 436 nm was reached after 18–20 h of growth. Cells were harvested by centrifugation and stored at −20 °C until use. The purification of cytochrome c_7 and 50 kDa cytochrome was performed as previously described [10].

2.2. Molecular mass determination

MALDI-MS was performed on a reflexion time of flight mass spectrometer equipped with delayed extraction (Voyager DE-RP, Perceptive Biosystems Inc.). In order to evaluate their respective response in MALDI-MS, analyses were performed separately for solutions of the holoprotein and of the apoprotein. Then, these solutions were mixed in suitable proportions and the resulting mixture analyzed. In each case, 0.7 μl of sample was directly mixed on the support with an equal volume of matrix (saturated solution of sinapinic acid in acetonitrile (40%), water with 0.1% of trifluoroacetic acid (60%)).

2.3. Temperature dependence of cytochrome c_7 polymerisation

The temperature dependence of cytochrome c_7 polymerisation was studied by heating 100 μl of the cytochrome c_7 solution (2.7 mg/ml, pH 7) at 1 K/min. Aliquots were taken at 20, 40, 60 and 90 °C, immediately cooled to 4 °C and then resolved at 15 °C by native PAGE on 12% polyacrylamide gels (Phast System Pharmacia). Gels were stained with Coomassie blue.

2.4. Spectroscopic methods and redox titration

Optical spectra were measured at 20, 40, 60 and 70 °C using a Kontron Uvicon XX spectrophotometer. Optical redox titrations were performed according

to Dutton [13] at pH 7.6, in 100 mM Tris–HCl buffer. Samples were kept under an argon atmosphere at 20 and 40 °C. The following redox mediators were present at a concentration of 2 μM: 1,4-benzoquinone, 2, 5-dimethyl-*p*-benzoquinone, 1,4-naphtoquinone, methylene blue, menadione, 2,5-dihydroxy-*p*-benzoquinone, 2-hydroxy-1,4 naphtoquinone, anthraquinone-2, 6-disulfonate, anthraquinone-2-sulfonate, safranine, neutral red, methylviologen for 50 kDa cytochrome (0.25 mg/ml) and 2,5-dihydroxy-*p*-benzoquinone, 2-hydroxy-1,4-naphtoquinone, anthraquinone-2,6-disulfonate, anthraquinone-2-sulfonate and safranine for concentration of cytochrome c_7 (0.25 mg/ml).

2.5. Amino acid analysis and protein sequencing

For the amino acid analysis, protein samples were hydrolyzed in 200 μl of 6 M HCl at 110 °C for 24 and 72 h in tubes sealed under vacuum and then analyzed with a Beckman amino acid analyzer (System 6300). Heme was removed using Ambler's method [14] and the resulting apoprotein was isolated by gel filtration on Sephadex G25 in 5% (v/v) formic acid. Sequence determinations were carried out on the apoprotein with an Applied Biosystems gas-phase sequenator (Models 470 A and 473 A). Quantitative determinations were performed on the phenyl thiohydantoin derivatives by means of high-pressure liquid chromatography (Waters Associates Inc.) monitored by a data and chromatography control station (Waters 840). *S*-carboxymethylated protein was prepared by dissolving the apoprotein in 0.5 M Tris–HCl (pH 9.0), 8 M urea and 20 mM EDTA, and treating it with iodoacetic acid, as described in [15]. This analysis was used to determine the protein concentration for the evaluation of the number of hemes.

2.6. Analysis for iron, selenium and heme content

The iron and selenium content was determined by plasma emission spectroscopy with a Jobin Yvon model JY 38 apparatus. The total number of heme units was determined by the pyridine ferrohemochromogene test [16].

2.7. Circular dichroism

CD spectra were recorded on a Jasco J-715 spectropolarimeter equipped with thermostated water-jacketed cells and a Neslab RTE-111 water bath and on a Jobin Yvon CD-6 dichrograph. The instruments were calibrated with standard nonhydroscopic ammonium (+)-10-camphorsulfonate, assuming a molar ellipticity $[\Theta]_{290.5}$ of 7910° $cm^2\,dmol^{-1}$ [17]. The cells had a light path of 0.02 and 0.1 cm, and protein concentration was 0.2–0.6 mg/ml. Protein solutions were prepared in 100 mM Tris–HCl buffer at pH 7.6. For continuous melting of the samples, the temperature was increased at a rate of 1 K/min and the denaturation temperatures were determined from the peaks on the first temperature derivatives of the melting profiles (accuracy ±0.5 °C for c_7 and ±1 °C for 50 kDa cytochrome). The results were expressed as molar circular dichroic absorption using $\Delta\varepsilon = \theta/33cl$, where c is the molar protein concentration, l the light pathlength in centimeters, and θ the measured ellipticity in degrees.

2.8. Differential scanning microcalorimetry

Microcalorimetric measurements were carried out on a DASM-4 microcalorimeter (NPO Biopribor, Pushchino, Russia) in 0.48 ml cells and on a MicroCal VP-DSC instrument (USA) in 0.51 ml cells at a heating rate of 1 K/min on 1.4–2.9 mg/ml cytochrome c_7 and 1.2–2.5 mg/ml 50 kDa cytochrome in 100 mM Tris–HCl buffer at pH 7.6. Protein solutions were extensively dialyzed before measurements against this buffer at 4 °C during 24 h. Curves were corrected for the instrumental baseline obtained by heating the solvent used for protein solution. The reversibility of denaturation was checked routinely by sample reheating after cooling in the calorimetric cell. The denaturation temperature (T_d), calorimetric denaturation enthalpy and vant't Hoff denaturation enthalpy were determined as described elsewhere [18]. To analyze functions of excess heat capacity, MicroCal Origin (4.1) software was used. The accuracy of the calorimetric denaturation enthalpy was ±6%, that of T_d within ±0.3 °C.

3. Results and discussion

3.1. Number of hemes in the 50 kDa cytochrome

The 50 kDa cytochrome is a slightly acidic protein (pI 6.55), purified as oligomers (250 kDa) [10]. The mass spectra showed that the subunit has a molecular

mass of 51240 Da. The number of heme groups which was found to be four per subunit in our previous publication [10] and six per subunit in the publication of Pereira et al. [11] was determined again. The iron content as determined by plasma emission spectroscopy was of 4 (±0.179) atoms of iron/molecule. The number of heme groups using the millimolar absorbance coefficient of 29.1 at the peak of the ferrohemochrome was calculated to be four (experimental value 3.8). The concentration of the protein solution in each analysis was determined by performing quantitative amino acid analysis. The molecular mass of the apoprotein (48858.8 ± 79.4 Da) has been compared to the molecular mass of the native protein (51240 ± 77 Da). The mean of five separate measurements on the same samples showed a mass difference of 2399 ± 26.2 Da between the holo- and apo-proteins and the molecular mass expected for four hemes is 2466 Da. The difference found corresponds to the removal of four hemes (experimental value 3.9). These results are in agreement with our previous characterization [10]. Furthermore, using plasma emission spectroscopy we have determined the presence of 1 ± 0.1027 selenium atom per subunit. The *N*-terminal amino acids determined up to the 30th residue were identical in the two publications [10,11], suggesting the identity between the two described cytochromes.

3.2. Heme core organization in cytochrome c_7 and 50 kDa cytochrome according to CD

Oxidized cytochrome c_7 displayed strong exitonic couplet in the Soret region, with a positive maximum at 403 nm, a negative minimum at 418 nm, and two α-helical type minima at 206 and 220 nm in the far-UV region (Fig. 1A). CD of cytochromes in the Soret region varies from a single positive band to spectra of varying degrees of complexity in sign and magnitude [19]. For each heme, there are two splitting components of the Soret band which have rotational strengths (CD amplitudes) of opposite sign. The shape of the Soret CD band depends on the orientation of the transition dipole moments of the two components in the heme plane [20]. It is known that the secondary and tertiary structure elements of three-heme cytochrome c_7 are highly homologous to those of cytochrome c_3 from *Desulfovibrio* with four hemes. Although the cytochrome c_7 lacks heme II,

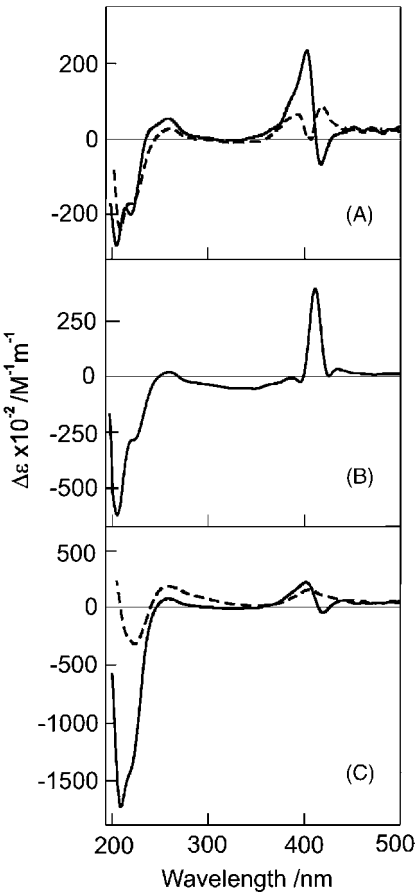

Fig. 1. CD spectra of oxydized cytochromes c_7 (A), c_3 from *Desulfovibrio vulgaris* Hildenborough (B) and 50 kDa cytochrome (C) at pH 7.6 at different temperatures: 10 °C (solid line), 90 °C (dashed line).

the remaining three have a relative arrangement similar to that reported for c_3 [6]. To compare the heme core structure in the cytochromes c_7 and c_3 by CD (Fig. 1A and B) we used the ratio between amplitudes of the Soret maximum and the far-UV CD minimum: this ratio appeared to be close in both proteins. This fact is indicative of the similarity of the heme core organization in these cytochromes which is in total agreement with the 3-dimentional structure of the two cytochromes [2,3,6].

Tetraheme 50 kDa cytochrome displays a positive CD maximum at 402 nm and a weak negative minimum at 419 nm in the Soret region and two α-helical minima at 208 and 222 nm in the far-UV region (Fig. 1C). Contrary to c_7, the ratio between the Soret

positive signal and the far-UV CD signal is much smaller for 50 kDa cytochrome than the corresponding ratio for cytochrome c_3. This suggests different surroundings of the hemes in 50 kDa cytochrome as compared with cytochrome c_3. In the CD spectrum of the temperature-denaturated 50 kDa cytochrome, a single positive band in Soret region is produced (Fig. 1C, dashed line). Taking into account the large number of aromatic amino acid residues in this cytochrome [10], it is quite probable that the remaining heme optical activity is the result of coupling of electronic π–π^* transitions between these aromatics and hemes [20].

3.3. Thermal denaturation of cytochromes c_7 and 50 kDa

Thermal denaturation of cytochromes was monitored by DSC, which is a direct method to probe the global protein stability, and by CD at 222 nm, reflecting the stability of the secondary structure, and at the Soret region, which is indicative of destruction of the anisotropy of the heme core environment.

Co-operative melting of tertiary and secondary structures of cytochrome c_7 takes place at similar temperatures, whereas the heme core structure is an additional stable for 2–3 °C (Fig. 2, Table 1). These data testify that the local heme core structure is the most rigid structural element. The partial molar heat capacity at 20 °C of cytochrome c_7, 0.92 J K^{-1} g^{-1}, is significantly lower than that of globular proteins of a comparable size and points to its lower flexibility. At 90 °C, the far-UV CD spectrum changes only slightly, i.e. the α-helical secondary structure is significantly retained (Fig. 1A, dashed line). The heat denaturation of cytochrome c_7 is irreversible and scanning calorimetry shows signs of aggregation after the transition peak. The ratio of calorimetric versus van't Hoff enthalpy is significantly below one indicating self-association of protein molecules in the course of heating. This result is in accordance with the native PAGE experiments with cytochrome c_7 at various temperature. At 20 °C, cytochrome c_7 is a monomer. An increase of temperature till 40 °C induced the appearance of a second band corresponding to a polymerized state of the cytochrome (data not shown). Aliquots taken at 60 and 90 °C showed the same electrophoretic pattern as that obtained at 40 °C. This association, probably, prevents complete unfolding and explains the low value of the denaturation enthalpy (only 105 kJ mol^{-1}) and preservation of a significant portion of secondary structure at 90 °C. To our surprise, despite the high level of structural similarity between cytochromes c_3 and c_7, the latter is 54 °C less stable [21]. Therefore, the presence of the cavity produced by the missing heme II in cytochrome c_7 leads to the sharp decrease of its thermostability compared to cytochrome c_3, which exhibits a high stability to temperature denaturation (until 121 °C

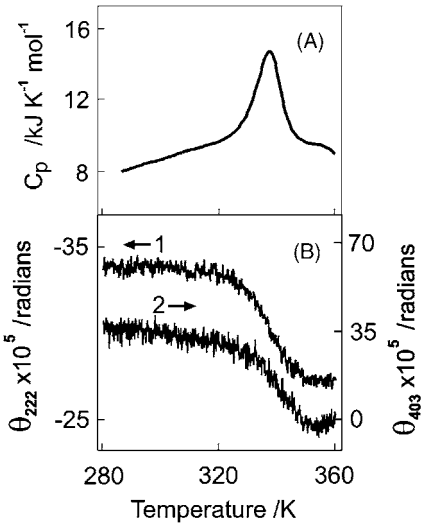

Fig. 2. Thermal denaturation of cytochrome c_7 at pH 7.6: (A) temperature dependence of the partial molar heat capacity; (B) temperature dependence of decrease in CD intensity at 222 nm (1) and at the maximum of the Soret band 403 nm (2).

Table 1
Thermal denaturation temperatures of cytochromes c_7 and 50 kDa cytochrome c at pH 7.6 determined by DSC and CD

Cytochrome	DSC	CD	
	T_d (°C)	T_d (°C) at 222 nm	T_d (°C) at Soret band
c_7	67.6	69	71[a]
50 kDa	36/64[b]		37/60[c]

[a] Denaturation temperature was determined by the change in the Soret maximum (403 nm) and minimum (418 nm).

[b] Temperatures were obtained from computer deconvolution of the transition excess heat capacity into two non-two-state transitions.

[c] Transition at 37 °C is revealed both by changes in the Soret band minimum (419 nm) and maximum (402 nm), whereas the transition at 60 °C is registered only by the change of the band minimum.

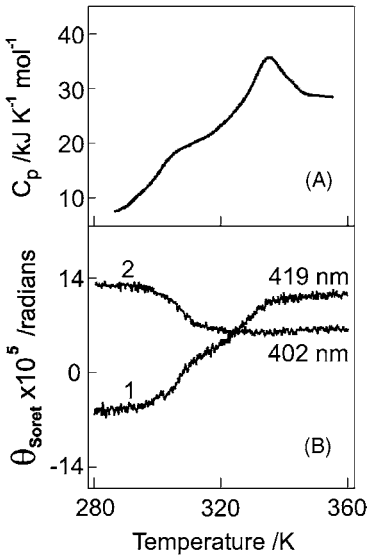

Fig. 3. Thermal denaturation of 50 kDa cytochrome at pH 7.6: (A) temperature dependence of the partial molar heat capacity; (B) temperature dependence of changes in CD intensity at the Soret band minimum (419 nm) (1) and maximum (402 nm) (2).

for *D. vulgaris* Hildenborough cytochrome c_3 [21]). An analogous decrease in the phage T4 lysozyme stability produced by cavity-creating mutations was observed in [22]. The destabilization of the mutant proteins increased in proportion to the cavity size.

The calorimetric melting curve of 50 kDa cytochrome consisted of two transitions at 36 and 64 °C (Fig. 3A), with the enthalpies of 142 and 460 kJ mol^{-1} (calculated per monomer), respectively. The CD also registered two co-operative transitions (Fig. 3B), the first of which coincides with the lower-temperature DSC peak, whereas the temperature of the second was close to that of the main DSC transition (Table 1). These data indicate the presence of two domains in 50 kDa cytochrome with significantly different intrinsic stabilities. The recently solved three-dimensional structure of a nine-heme cytochrome, which is related to cytochrome c_3 and high-molecular mass cytochrome (Hmc) family from *Desulfovibrio* points out to the presence of two domains in the molecule [5]. The same structural organization might be found in 50 kDa cytochrome, which agrees with the calorimetric data. The data obtained show that all four hemes of 50 kDa cytochrome contribute to the Soret band minimum in the CD spectrum, whereas only a single heme of which the local structure melted in the low-temperature peak contributes to the band maximum.

3.4. Optical spectra and redox titration

For cytochrome c_7, till 70° C, no modification of the optical spectra or the redox potential (−102 mV (one heme), −177 mV (two hemes) [6]) were observed. The UV–VIS spectra of the reduced 50 kDa cytochrome at 40 °C showed a diminition of the peak at 552 nm of around 30% (Fig. 4A) compared to the optical spectra at 20 °C. At 20 °C, three distinct redox centers (around −364 ± 19 mV (two hemes); −162 ± 18 mV (one heme) and 94 ± 10 mV (one heme) (Fig. 4B) appeared to be involved in the electron transfer of the 50 kDa cytochrome. The heme with the redox potential of 94 mV presents its maximum absorption at 554 nm compared to 552 nm for the other two (inset of Fig. 4A). At 40 °C only two distinct redox centers (−332 and 126 mV) were detected in the redox potential range studied (Fig. 4B). This result is in accordance with the optical spectra at 40 °C. The loss of the redox center (−162 mV) was caused by unfolding and/or conformational changes of the heme microenvironment inducing the exposure of the heme to the solvent. The above-described thermal denaturation experiments demonstrate the presence of two domains in the 50 kDa cytochrome. At 40 °C, only three hemes out of four are detected in the range redox potentials studied. Hence, the domain with a lower transition temperature contains only one heme, whereas the higher-temperature domain contains the other three hemes. This corresponds to the ratio of the denaturation enthalpies of the second-to-first calorimetric peaks, which is also equal to three.

All the multihemic cytochromes already described in sulfate and sulfur reducing bacteria belong to the cytochrome c_3 superfamily in regard to the presence of several hemes in the same molecule with a bishistidinyl iron coordination and low redox potential. Using site-directed mutagenesis, the thermal stability of this class of cytochromes has been demonstrated to be directly linked to the presence of the histidine as sixth axial ligand [23]. On the basis of the core folding, the thermal resistance and the presence of domains, we propose to divide this family in two sub-groups. Cytochrome c_3 and cytochromes formed by the association of cytochrome c_3-like domains

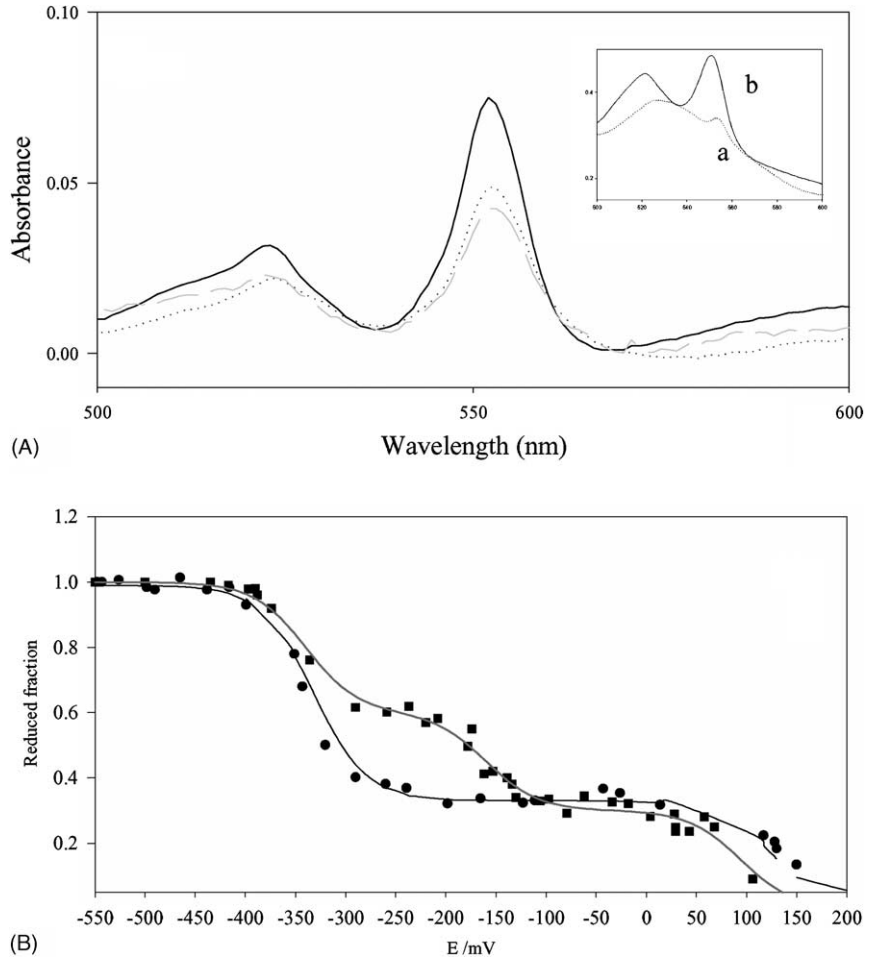

Fig. 4. (A): Visible optical spectra of reduced (dithionite) 50 kDa cytochrome *c* at 20 °C (solid line), 40 °C (dotted line) and 60 °C (dashed line). The insert shows the optical spectra at 80 (a) and −340 mV (b). (B): Redox titration of the α-band amplitude of the 50 kDa cytochrome by performing optical absorbance measurements at 553 nm at 20 °C (■) and 40 °C (●). Solid lines give the best fit between the data and the Nernst curves.

form the first group. Eight-heme cytochrome c_3 and triheme cytochrome c_7, which has been demonstrated to have a cytochrome c_3-like fold, belong to this group. The nine-heme cytochrome from *Desulfovibrio desulfuricans* is the first known structure where multiple copies of a tetraheme cytochrome c_3-like fold are present in the same polypeptide chain of 37.3 kDa. It consists of two domains connected by a 34-residue long polypeptide segment [5] and can be connected to this first group. Recent results on nonaheme cytochrome *c* from *D. desulfuricans* Essex showed the structural homology with cytochrome c_3 folding [24] and similar reactivity with hydrogenase. Considering these similarities we propose to connect these two nineheme cytochromes be connected to this first group. However, in the evolutionary pathway for the structural scaffolding of this super family, several processes of gene duplication, fusion and modification could occur leading to more complex structures. These structures are evolutionarily based on the common tetraheme motif as building block but other heme containing domains could also occur. For example, it has been proposed that the structure of the 16-heme high molecular weight cytochrome from *D. vulgaris* (strains Miyazaki and Hildenborough) and *D. gigas* is formed by the combination of

three tetraheme, one triheme and one single heme motifs in a molecule of 65.6 kDa. Contrary to the first group, this cytochrome is not efficiently reduced by hydrogenase [25]. The redox potentials are distributed in three different ranges 0, −100 and −250 mV due to the presence of one or two high spin hemes and 14 or 15 low spin hemes associated in domains. The denaturation temperature of *DvH* Hmc is 40 °C less than that of *DvH* cytochrome c_3 [26]. In the case of the 50 kDa cytochrome from *D. acetoxidan*s, we observe like in Hmc, three distinct redox type centers and no reactivity with hydrogenase [27]. On the basis of our results on 50 kDa *D. acetoxidans* cytochrome (no aminoacid sequence or functional homology with the first group of cytochrome, organization in two domains both less thermostable than the cytochrome c_3-like fold) we propose to classify this cytochrome and also the 65 kDa cytochrome in a second group of the cytochrome c_3 family. Moreover, the recent characterization of low potential monohemic cytochrome from *Synechocytis* [28] and multihemic cytochromes *c* in Purple Phototropic Bacteria [29] with two histidines as heme ligands and both bearing no relationships to class I and class III *c*-type cytochromes raises the possibility to create a new subgroup in the class III. With the growing numbers of bacteria genomes sequenced, as soon as their annotation will be done, the analysis of the various classes of *c*-type cytochromes would be revised.

Acknowledgements

We gratefully acknowledge the contribution of R. Toci (Fermentation Plant Unit L.C.B., Marseilles France) for growing the bacteria, M. Woudstra for cytochrome purification, G. Leroy for redox titration and J. Bonicel (Protein sequencing Unit, B.I.P., Marseilles, France) for mass spectrum determination and Pr G. Voordouw for his critical reading of the manuscript. This work was supported by the PICS 486 from CNRS and the RFBR-CNRS 98-04-22001 from the Russian Foundation of Basic Research.

References

[1] G.R. Moore, G.H. Pettigrew, Cytochromes *c*: evolutionary, structural and physicochemical aspects. Springer, Berlin, Heidelberg, New York, 1990, p. 241.
[2] J.B. Coutinho, A.V. Xavier, Methods Enzymol. 243 (1994) 119.
[3] M. Czjzek, F. Payan, F. Guerlesquin, M. Bruschi, R. Haser, J. Mol. Biol. 243 (1994) 653.
[4] M. Czjzek, F. Guerlesquin, M. Bruschi, R. Haser, Structure 4 (1996) 395.
[5] P.M. Matias, R. Coelho, I. Ac Pereira, A.V. Coelho, A.W. Thompson, L.C. Siebsker, J. Le Gall, M.A. Carrondo, Structure 7 (1999) 119.
[6] L. Banci, I. Bertini, M. Bruschi, P. Sompornpisut, P. Turano, Proc. Natl. Acad. Sci. U.S.A. 93 (1996) 14396.
[7] D.L. Turner, H.S. Costa, I.B. Coutinho, J. Le Gall, A.V. Xavier, Eur. J. Biochem. 243 (1997) 474.
[8] W.B.R. Pollock, M. Loutfi, M. Bruschi, B.J. Rapp-Giles, J.D. Wall, G. Voordouw, J. Bacteriol. 173 (1991) 220.
[9] M. Bruschi, Methods Enzymol. 243 (1994) 140.
[10] M. Bruschi, M. Woudstra, B. Guigliarelli, M. Asso, E. Lojou, Y. Petillot, C. Abergel, Biochemistry 35 (1997) 10601.
[11] I.A.C. Pereira, I. Pacheco, M.Y. Liu, I. Le Gall, A.V. Xavier, M. Texeira, Eur. J. Biochem. 248 (1997) 323.
[12] N. Pfennig, H. Biebl, Arch. Microbiol. 110 (1976) 115.
[13] P.L. Dutton, Methods Enzymol. 54 (1978) 411.
[14] R.P. Ambler, Biochem. J. 89 (1963) 349.
[15] A.M. Crestfield, S. Moore, W.H.J. Stein, J. Biol. Chem. 238 (1963) 622.
[16] J.E. Falk, Porphyrins and Metalloporphyrins: Their General Physical and Coordination Chemistry and Laboratory Methods, Elsevier, New York, 1964, pp. 240.
[17] T. Takakuwa, T. Konno, H. Meguro, Anal. Sci. 1 (1985) 215.
[18] A.A. Makarov, I.I. Protasevich, E.G. Frank, I.B. Grishina, I.A. Bolotina, N.G. Esipova, Biochim. Biophys. Acta 1078 (1991) 283.
[19] M. Bruschi, P. Bertrand, C. More, G. Leroy, J. Bonicel, J. Haladjian, G. Chottard, W.B.R. Pollock, G. Voordouw, Biochemistry 31 (1992) 3281.
[20] M.-C. Hsu, R.W.J. Woody, Am. Chem. Soc. 93 (1971) 3515.
[21] A. Dolla, P. Arnoux, I. Protasevich, V. Lobachov, M. Brugna, M.T. Giudici-Orticoni, R. Haser, M. Czjzek, A. Makarov, M. Bruschi, Biochemistry 38 (1999) 33.
[22] A.E. Eriksson, W.A. Baase, X.-J. Zhang, D.W. Heinz, M. Blaber, E.P. Baldwin, B.W. Matthews, Science 255 (1992) 178.
[23] A. Dolla, L. Florens, M. Bruschi, I.V. Dudich, A.A. Makarov, Biochem. Biophys. Res. Commun. 211 (1995) 742.
[24] S. Umhau, G. Fritz, K. Diederichs, W. Welte, P.M.H. Kroneck, Biochemistry 40 (2001) 1308.
[25] C. Aubert, M. Brugna, A. Dolla, M. Bruschi, M.T. Giudici-Orticoni, Biochim. Biophys. Acta 1476 (1) (2000) 85.
[26] L. Florens, P. Bianco, J. Haladjian, M. Bruschi, I. Protasevich, A. Makarov, FEBS Lett. 373 (1995) 280.
[27] M. Brugna, W. Nitschke, R. Toci, M. Bruschi, M.T. Giudici-Orticoni, J. Bacteriol. 181 (17) (1999) 5505.
[28] C. Frazào, F.J. Enguita, R. Coelho, G.H. Sholdrick, J.A. Navarro, M. Hervas, M.A. De la Rosa, M.A. Carrondo, J. Biol. Inorg. Chem. 6 (2001) 324.
[29] B. Devreese, A. Brige, K. Backers, G. Van Driessche, T. Meyer, M. Cusanovich, J. Van Beemen, Arch. Biochem. Biophys. 381 (1) (2000) 53.